Intrinsic Network Activity in Tinnitus Investigated Using Functional MRI

Amber M. Leaver,[1,2]*† Ted K. Turesky,[1†] Anna Seydell-Greenwald,[1] Susan Morgan,[3] Hung J. Kim,[4] and Josef P. Rauschecker[1,5]*

[1]*Department of Neuroscience, Georgetown University Medical Center, Washington, District of Columbia*
[2]*Department of Neurology, University of California Los Angeles, Los Angeles, California*
[3]*Division of Audiology, Medstar Georgetown University Hospital, Washington, District of Columbia*
[4]*Department of Otolaryngology, Medstar Georgetown University Hospital, Washington, District of Columbia*
[5]*Institute for Advanced Study, TU Munich, Germany*

Abstract: Tinnitus is an increasingly common disorder in which patients experience phantom auditory sensations, usually ringing or buzzing in the ear. Tinnitus pathophysiology has been repeatedly shown to involve both auditory and non-auditory brain structures, making network-level studies of tinnitus critical. In this magnetic resonance imaging (MRI) study, two resting-state functional connectivity (RSFC) approaches were used to better understand functional network disturbances in tinnitus. First, we demonstrated tinnitus-related reductions in RSFC between specific brain regions and resting-state networks (RSNs), defined by independent components analysis (ICA) and chosen for their overlap with structures known to be affected in tinnitus. Then, we restricted ICA to data from tinnitus patients, and identified one RSN not apparent in control data. This tinnitus RSN included auditory–sensory regions like inferior colliculus and medial Heschl's gyrus, as well as classically non-auditory regions like the mediodorsal nucleus of the thalamus, striatum, lateral prefrontal, and orbitofrontal cortex. Notably, patients' reported tinnitus loudness was positively correlated with RSFC between the mediodorsal nucleus and the tinnitus RSN, indicating that this network may underlie the auditory–sensory experience of tinnitus. These data support the idea that tinnitus involves network dysfunction, and further stress the importance of communication between auditory–sensory and fronto-striatal circuits in tinnitus pathophysiology. *Hum Brain Mapp 37:2717–2735, 2016.*

Key words: auditory; functional connectivity; fMRI; striatum; thalamus; hearing loss

Additional Supporting Information may be found in the online version of this article.

Contract grant sponsor: National Institutes of Health; Contract grant number: RC1-DC010720; Contract grant sponsors: American Tinnitus Association and Tinnitus Research Consortium

*Correspondence to: Amber M. Leaver, 935 Charles E Young Dr S #225, University of California Los Angeles, Los Angeles, CA 90095. E-mail: aleaver@ucla.edu or Josef P. Rauschecker, 3970 Reservoir Rd NW, Georgetown University Medical Center, Washington, DC 20057. E-mail: rauschej@georgetown.edu

†Amber M. Leaver and Ted K. Turesky contributed equally to this work.

The authors report no financial conflict of interest.

Received for publication 22 May 2015; Revised 29 February 2016; Accepted 24 March 2016.

DOI: 10.1002/hbm.23204
Published online 19 April 2016 in Wiley Online Library (wileyonlinelibrary.com).

INTRODUCTION

Tinnitus is an auditory disorder characterized by ringing or buzzing that is perceived in the absence of an external sound source [Eggermont and Roberts, 2004; Møller, 2003]. Already, roughly 40 million people in the United States suffer from the disorder [Henry et al., 2005], and this number is expected to rise, as factors commonly associated with tinnitus (e.g., age-related and noise-induced hearing loss) also rise. Despite the prevalence of this disorder, tinnitus pathophysiology remains poorly understood. A large body of evidence has revealed that tinnitus is associated with changes in the auditory system, including functional and anatomical changes at one or more sites along peripheral or central auditory pathways [Eggermont and Roberts, 2004; Engineer et al., 2011; Gu et al., 2010; Jastreboff, 1990]. In addition, several studies have found tinnitus-related differences in non-auditory brain areas, notably, in structures constituting part of the limbic system [Eichhammer et al., 2007; Leaver et al., 2011, 2012; Lockwood et al., 1998; Mirz et al., 2000; Mühlau et al., 2006; Seydell-Greenwald et al., 2012; Shulman, 1995]. These data have spurred several models of tinnitus proposing significant roles for non-auditory brain regions in tinnitus pathophysiology [De Ridder et al., 2011a; Jastreboff, 1990; Mühlau et al., 2006; Rauschecker et al., 2010; Shulman et al., 2009; Vanneste and De Ridder, 2012]. Although the details of these models may differ, there does seem to be a consensus that chronic tinnitus involves deficits at the network level, rather than in a single structure. Thus, there is a need for studies measuring brain function at the network level in tinnitus.

Cross-sectional comparisons of intrinsic, or "resting-state," function are a common way of assessing how various disorders affect brain networks [Damoiseaux et al., 2012; Greicius et al., 2007; Raichle et al., 2001]. In these studies, brain activity is measured while volunteers rest and do not perform an experimental task [Power et al., 2010; Smith et al., 2009]. In this context, investigators can potentially capture brain activity related to the tinnitus percept itself, because patients' sensory-perceptual experience "at rest" (i.e., the tinnitus percept and its possible consequences) is quite different from that of control volunteers who do not experience tinnitus. Thus, resting-state functional connectivity (RSFC) research could improve upon task-based functional neuroimaging studies of tinnitus, which are restricted to making inferences regarding tinnitus-related activity with brain responses to experimentally presented sounds [Gu et al., 2010; Leaver et al., 2011; Melcher et al., 2000, 2009; Seydell-Greenwald et al., 2012].

Despite the obvious relevance of RSFC research to tinnitus, no clear picture of the networks affected has yet emerged. Resting-state fMRI, EEG, and MEG studies have identified altered function in several parts of the brain, including in auditory cortex [Burton et al., 2012; Kim et al., 2012; Maudoux et al., 2012a,b; Vanneste et al., 2011a,b], basal ganglia [Maudoux et al., 2012b], prefrontal cortex [Kim et al., 2012; Maudoux et al., 2012b; Schlee et al., 2009], parahippocampal regions [Maudoux et al., 2012a,b; Schmidt et al., 2013; Vanneste et al., 2011a], and insula [Burton et al., 2012; Vanneste et al., 2011b]. However, these results have been variable (e.g., see Husain and Schmidt [2014] for review), and other studies have found no differences in network processing between tinnitus patients and controls [Davies et al., 2014; Wineland et al., 2012]. For the corpus of resting-state EEG and MEG studies (for a review, see Vanneste and De Ridder [2012]), limited spatial resolution may have contributed to the observed variability, particularly in midline cortical and subcortical structures. In the resting-state fMRI literature, inconsistencies may stem from methodological differences; some studies used seed-based techniques to define networks of interest [Burton et al., 2012; Kim et al., 2012; Schmidt et al., 2013; Wineland et al., 2012], while others used independent component analysis (ICA) to define resting-state networks (RSNs, [Allen et al., 2011; Damoiseaux et al., 2006; Laird et al., 2011; Smith et al., 2009]) for comparison between tinnitus patients and controls [Davies et al., 2014; Maudoux et al., 2012a,b]. In nearly all studies, *a-priori* assumptions were made regarding what regions and RSNs were of interest to tinnitus. This high degree of variability underscores the need for further RSFC research.

In the current study, we implemented a comprehensive, data-driven approach using ICA to measure tinnitus-related disruptions in resting-state fMRI data. We acquired these data in patients with chronic tinnitus ($n = 21$) and in healthy controls ($n = 19$) matched for demographics (Table I) and mean hearing loss (Table 1 and Supporting Information Fig. S1). We had two main goals. First, we compared RSFC patterns in "typical" RSNs that have been well-characterized in previous resting-state fMRI studies using ICA [Allen et al., 2011; Damoiseaux et al., 2006; Laird et al., 2011; Smith et al., 2009] and that overlapped with brain regions previously associated with tinnitus. Second, because patients experienced tinnitus during fMRI scans while controls did not, we also searched for possible "atypical" RSNs specific to tinnitus patients that may better reflect tinnitus circuitry than "typical" RSNs. In both analyses, we measured the extent to which tinnitus-related effects of RSFC could be explained by hearing loss and/or behavioral symptoms of tinnitus (specifically, loudness and distress). In this way, we sought to further a network-level understanding of tinnitus pathophysiology.

MATERIALS AND METHODS

Participants

Forty volunteers (21 tinnitus patients, 19 controls) gave informed consent to participate in this study according to procedures of the Institutional Review Board at Georgetown University and the Code of Ethics of the World

TABLE I. Participant characteristics

Participant	Sex	Age (years)	HL, mean (dB HL)	LDL, 1kHz (dB HL)[a]	GAD-7	TF (Hz)	THI	Pre-scan loudness	Postscan loudness	Tinnitus onset (years ago)	Tinnitus ear
Patient 1	f	57	46.25	78	2	8,484	8	5	6	5.00	Bilateral
Patient 2	f	56	30.54	94	7	1,605	12	1	7	7.00	Bilateral
Patient 3	f	66	34.58	77	3	5,297	38	1	3.5	1.00	R
Patient 4	f	28	17.33	80	3	1,894	32	4	3	1.50	L
Patient 5	f	60	48.27	≥100	4.5	5,000	34	7	8	10.50	Bilateral
Patient 6	m	65	43.21	96	3	5,946	14	3	3	0.75	Bilateral
Patient 7	m	65	38.96	84	3	4,413	40	5	7	25.00	Bilateral
Patient 8	m	64	33.75	88	1	1,388	12	5	6	4.00	Bilateral
Patient 9	m	62	49.04	≥100	2	819	20	3	4	5.00	Bilateral
Patient 10	f	33	7.17	85	6	1,214	18	7	9	5.00	Bilateral
Patient 11	m	45	33.04	88	0	726	2	4	4	0.33	Bilateral
Patient 12	f	48	36.07	≥100	2	10,617	14	2	5	2.00	Bilateral
Patient 13	m	34	14.67	≥100	8	7,681	20	1	4	22.00	Bilateral
Patient 14	f	38	52.32	88	11	3,929	88	8	7	1.25	Bilateral
Patient 15	f	49	32.86	85	17	2,630	70	5	9	1.16	L
Patient 16	f	47	29.17	91	6	1,644	28	2	5	21.50	Bilateral
Patient 17	m	43	40.36	97	2	8,044	30	3	7	7.00	Bilateral
Patient 18	f	32	16.96	91	0	2,802	37	3	2	16.50	R
Patient 19	m	42	21.17	84	2	4,410	14	2	4	4.00	Bilateral
Patient 20	m	37	14.33	88	7	6,243	50	4	6	11.00	L
Patient 21	m	23	13.17	98	0	3,177	0	3	4	3.00	Bilateral
Control 1	m	56	36.73	≥100	1.5						
Control 2	f	58	40.54	98	2						
Control 3	f	66	45.63	88	0						
Control 4	f	29	3.75	na	0						
Control 5	m	61	26.00	≥100	0						
Control 6	m	67	32.17	≥100	0						
Control 7	m	57	31.07	80	2						
Control 8	f	64	30.00	95	13						
Control 9	f	41	5.00	na	2						
Control 10	m	50	32.31	≥100	3						
Control 11	f	53	23.75	87	1						
Control 12	m	34	13.50	76	5						
Control 13	f	42	19.00	≥100	1						
Control 14	f	49	25.89	≥100	2						
Control 15	f	53	22.68	96	0						
Control 16	m	46	19.64	≥100	7						
Control 17	f	30	13.39	89	4						
Control 18	m	46	25.96	97	0						
Control 19	m	27	4.50	≥100	5						
Patients, mean	11f,10m	47.33	31.11	90.05	4.26	4,188.71	27.67	3.71	5.40	7.36	
Patients, SD	n/a	13.47	13.38	7.49	4.12	2,828.64	21.70	2.00	2.01	7.63	
Controls, mean	10f,9m	48.89	23.76	94.44	2.55						
Controls, SD	n/a	12.49	11.91	7.71	3.24						
P-value[b]	1.00	0.71	0.08	0.08	0.16				0.0004		

Abbreviations: HL, hearing level; LDL, loudness discomfort level; GAD-7, generalized anxiety disorder scale; TF, tinnitus frequency; THI, tinnitus handicap inventory; n/a, not applicable; na, not acquired.

[a]LDL tests were typically aborted by the audiologist at 100 dB HL.

[b]Chi-squared tests compared gender distributions between groups; unpaired *t*-tests compared groups on other measures. Pre- and post-scan loudness scores were compared with paired *t*-tests.

Medical Association (Declaration of Helsinki). Participants were recruited using flyers posted on the campuses of Georgetown University Medical Center and MedStar Georgetown University Hospital, as well as with advertisements in local newspapers. Patient and control participants were matched by age and sex, and standard MRI safety

considerations were used as exclusion criteria. In total, 24 patients and 21 controls participated in behavioral and MRI sessions; however, three patients and two controls were excluded from analyses due to motion and/or poor image quality and are not discussed here. Detailed characteristics of the final cohorts can be found in Table I. Other MRI data from this same cohort have been presented previously [Leaver et al., 2012; Seydell-Greenwald et al., 2012, 2014]; differences in sample size are due to different quality control measures implemented for different MRI modalities.

Audiometry

Audiometric testing assessed pure-tone thresholds in all participants at the Division of Audiology at Georgetown University. Frequencies ranging from 250 Hz to 20 kHz were presented to each ear until detection thresholds were reached. Table I lists mean hearing levels for each volunteer (calculated using all test frequencies), and Supporting Information Figure S1 displays hearing levels for each group averaged across ears at each test frequency. Tinnitus patients had experienced tinnitus for at least four months [mean (SD) = 7.4 (7.6) years]. Loudness discomfort levels (LDL) were assessed using 1-kHz pure tones presented at increasing amplitudes until the subject indicated discomfort, or once the amplitude reached 100 dB HL. LDLs are listed in Table I. Neither according to this quantitative measure, nor in response to questions about noise sensitivity on the Tinnitus Sample Case History Questionnaire (TSCHQ, [Langguth et al., 2007]), did any of the participants classify as suffering from hyperacusis or phonophobia. In-house MATLAB (The MathWorks, Inc.) scripts allowed patients to adjust the frequency, right-left balance, bandwidth, and intensity of a test tone to match their tinnitus; best frequency-match to dominant tinnitus pitch was high [mean (SD) = 4,189 (2,829) Hz], and most reported bilateral tinnitus ($n = 16$).

Behavioral Assessments

Participants completed a brief battery of questionnaires. Among these were the Generalized Anxiety Disorder scale (GAD-7), Hospital Anxiety and Depression Scale (HADS), and Patient Health Questionnaire (PHQ-9), which assessed symptoms of depression and anxiety. These measures were intercorrelated for all subjects; thus, we report only the GAD-7 anxiety metric in the current article. Tinnitus patients also completed the Tinnitus Handicap Inventory (THI) to measure tinnitus impact or distress [Newman et al., 1996] and a questionnaire that assessed subjective tinnitus loudness on a 10-point scale administered before and after scanning. Behavioral measures are listed for each volunteer in Table I.

MRI Acquisition and Preprocessing

Images were acquired using a 3.0 Tesla Siemens TIM Trio scanner with a 12-channel head coil. High-resolution anatomical scans (MPRAGE) were acquired with the following parameters: TR = 2,530 ms, TE = 3.5 ms, inversion time = 1,100 ms, flip angle = 7°, 176 sagittal slices, matrix size 256 × 256 mm^2, 1 × 1 × 1 mm^3 resolution. The parameters for functional echo-planar images (EPIs) were: 200 volumes, TR = 1,500 ms, TE = 30 ms, flip angle = 90°, FOV = 192 mm, 64 × 64 matrix, 28 transverse slices of 3.5 mm thickness, resulting in functional voxels of 3 × 3 × 3.5 mm^3. Two additional EPI volumes were acquired and discarded prior to the EPI scan to accommodate T1 stabilization. To reduce signal loss due to susceptibility artifacts in orbitofrontal cortex, EPI slices were rotated 30° clockwise from the ACPC plane [Deichmann et al., 2003; Weiskopf et al., 2006]. MR images were preprocessed using BrainVoyager QX (Brain Innovation, Inc.). Functional images were corrected for slice acquisition time, motion and linear trend, and smoothed with a 6-mm isotropic Gaussian kernel (measured at full width half maximum, FWHM). Because ICA identifies sources of temporal noise that are spatially consistent (e.g., due to motion and vasculature; [Perlbarg et al., 2007; Salimi-Khorshidi et al., 2014]), additional temporal filtering was not applied. Functional and anatomical images were aligned and normalized [Talairach and Tournoux, 1988] using a linear transformation. During normalization, functional images were interpolated to 3 × 3 × 3 mm^3 resolution. Slice rotation during acquisition limited the field of view in superior–posterior cortex in some volunteers (mostly excluding superior parietal cortex); therefore, statistical analyses were performed only using those voxels that overlapped with the normalized brains of all participants (Supporting Information Fig. S2).

Independent Component Analysis (ICA)

Group connectivity analyses were performed using ICA implemented in BrainVoyager QX, and three concatenated [Calhoun et al., 2001; Erhardt et al., 2011; Filippini et al., 2009] data sets were analyzed: (1) patients and controls to identify and compare typical networks common to both groups, (2) tinnitus patients only to identify networks unique to the tinnitus disorder, and (3) controls only for comparison with the networks identified in the tinnitus-only analysis. In all three cases, ICA was applied using the same protocol, which is illustrated in Supporting Information Figure S3. First, single-subject images were temporally z-normalized, concatenated in Matlab with the NeuroElf toolbox (www.neuroelf.net), and analyzed with BrainVoyager's ICA plugin [Formisano et al., 2004], which implemented the FastICA algorithm [Hyvarinen, 1999] with a deflation approach, tanh nonlinearity function, and 25 eigenvalues (and thus 25 components). Twenty-five was chosen as the target number of independent components (ICs) in line with previous work [Greicius et al., 2007]. In

this approach, the temporal dimensionality of concatenated data was first reduced using principal components analysis (PCA), and then ICA was used to identify ICs.

The stochastic nature of data-fitting in ICA [Hyvarinen, 1999] is such that the ICA algorithm may define ICs differently each time it is applied to the same dataset. For example, a given IC may be present or absent, may be split into multiple ICs, or combined with other ICs, across repeated ICA on the same dataset [Allen et al., 2011; Damoiseaux et al., 2006; Laird et al., 2011; Smith et al., 2009; Uddin et al., 2009]. Thus, we ran ICA ten times for each of the three concatenated datasets (listed above) and, for all subsequent analyses, we targeted RSNs that were present in at least 7 out of 10 iterations of ICA. ICs were matched and sorted into "IC-aggregates" based on the similarity of their power spectra using hierarchical clustering in Matlab's Statistics Toolbox. Hierarchical clustering was chosen because we did not necessarily expect a given IC to be present or "intact" each time ICA was applied to the data [Hyvarinen, 1999]. Power spectra were used to obviate the need to match signed (positive or negative) relationships between ICs during clustering. First, pairwise similarities in IC-timecourse power spectra were computed using Pearson's correlation; then, average Euclidean distance measured the hierarchical relationships between IC-timecourse power spectra; and finally ICs were clustered at $r > 0.90$ (Supporting Information Fig. S4). The criterion $r > 0.90$ was chosen because it maximized the number of IC-aggregates containing at least 7 ICs. (Note that two IC-aggregates consisted of 11 ICs; these contained two ICs from the same iteration.) IC spatial maps were examined to confirm spatial overlap, matched for sign, and converted to a single binarized IC-aggregate map that reflected whether each voxel was functionally correlated with that network ($z > 2.81$, $P < 0.005$) in at least 7 of 10 ICA iterations. IC-aggregate maps are shown in Supporting Information Figure S5.

IC-timecourses corresponding to each IC-aggregate were also averaged for use in region-of-interest (ROI) analyses and group comparisons using the GLM as described further below. Partial correlation analyses estimated the variance explained by each IC-aggregate timecourse, after removing variance associated with all other IC-aggregate timecourses and subjects. In Supporting Information Figure S5, we report partial correlation values for each IC-aggregate, averaged across all voxels in the brain. Power spectra for averaged IC-timecourses can be found in Supporting Information Figure S6. Thus, each IC-aggregate reflects a specific functional RSN, differentiable from other functional networks, and consistent across ICA iterations. Throughout the main manuscript, we refer to these IC-aggregate networks simply as RSNs.

Statistical Analyses of Typical RSNs

To test for group differences in well-characterized RSNs common to both groups [see e.g., Allen et al., 2011; Damoiseaux et al., 2006; Laird et al., 2011; Smith et al., 2009], we performed direct statistical comparisons of RSNs defined using the concatenated dataset comprising all participants. RSN timecourses were separated for each subject, and used as regressors in a random-effects GLM including all RSNs and all subjects. To attempt to reduce the probability of Type I error, only RSNs that included regions previously implicated in tinnitus were targeted for comparisons between groups (*t*-tests). These included networks overlapping with the auditory system [Gu et al., 2010; Leaver et al., 2011; Melcher et al., 2000, 2009; Seydell-Greenwald et al., 2012, 2014], ventromedial prefrontal and anterior cingulate cortex [Boyen et al., 2013; Leaver et al., 2011, 2012; Seydell-Greenwald et al., 2012]), striatum [Cheung and Larson, 2010; Leaver et al., 2011; Maudoux et al., 2012b], thalamus [Mühlau et al., 2006], and posterior cingulate cortex (part of the default mode network with medial prefrontal and anterior cingulate cortex [Maudoux et al., 2012a]). A single-voxel threshold was set at $P_{\text{uncorr}} < 0.0005$, with a cluster correction for family-wise error using random field theory [$P_{\text{corr}} < 0.05$, $k > 12$; Poline et al., 1997]. In clusters resulting from these between-groups *t*-tests, ROI analyses were also performed to measure correlations between network connectivity values and: (1) pre-MRI tinnitus loudness, (2) post-MRI tinnitus loudness, (3) tinnitus distress (with THI values), (4) mean hearing loss, and (5) anxiety (with GAD-7 values). Correlations were considered significant at $r = \pm 0.549$, $P < 0.01$, Bonferroni-corrected for the five tests performed in each RSN and group.

Statistical Analyses of Atypical RSNs

RSNs (i.e., IC-aggregates as described above) were identified using ICA separately for tinnitus patients and controls to distinguish RSNs common to both groups and unique to either group. The spatial similarity of these RSNs was then compared to identify functional networks common to both groups and networks unique to either group. RSNs were compared using spatial cross-correlation and hierarchical clustering in Matlab. Spatial (vs. spectral/temporal) relationships were used for this analysis because we were most interested in brain-regional differences between groups (as opposed to spectral/temporal differences). First, maps where the majority of thresholded voxels did not overlap with gray matter were removed, yielding 15 IC maps per group. Then, the remaining maps were imported into Matlab using NeuroElf, and spatial similarity was computed for each pair of maps using Pearson's *r*. Cluster analysis was performed using Matlab's Statistics Toolbox, with average Euclidean distance determining the hierarchical relationships between maps. A threshold of $r > 0.03$ was chosen to group spatially similar networks for easy visualization in a dendrogram and figures, and is not meant to indicate statistically meaningful groupings.

RSN maps with limited spatial similarity to other RSNs were deemed atypical and potentially unique (max pairwise correlations $r < 0.10$, mean pairwise correlation $r < 0.001$); a single atypical network identified in tinnitus patients was targeted for further analysis. To extract values for ROI analyses, RSN timecourses were first separated for each subject, and these timecourses were used as regressors in a random-effects GLM analysis in tinnitus patients. Resulting clusters represented regions of the brain that were strongly correlated with the RSN timecourse and therefore reflected network connectivity values. These clusters were subsequently defined as ROIs, and mean connectivity values in each ROI were tested for correlations with behavioral variables, including: (1) pre-MRI tinnitus loudness, (2) post-MRI tinnitus loudness, (3) tinnitus distress (with THI values), (4) mean hearing loss, and (5) anxiety (with GAD-7 values). Again, correlations were considered significant at $r = \pm 0.549$, $P < 0.01$, Bonferroni-corrected for the five tests performed in each network.

Exploratory Analyses of Potential Atypical RSNs

In potentially atypical RSNs identified only in tinnitus patients, we performed exploratory connectivity analyses using the "raw" intrinsic fMRI signal from regions composing these networks (i.e., preprocessed timecourses not derived from ICA). In this way, we were able to compare functional connectivity of the regions in these tinnitus-unique networks between both tinnitus patients and controls. Note, however, that this analysis captures a different aspect of functional connectivity than ICA; while ICA measures temporal coherence between regions and RSNs with temporal variability associated with other RSNs and ICs removed, this ROI–ROI analysis measures temporal coherence between ROIs with removal of relatively fewer sources of temporal variability. Specifically, we: (1) calculated the mean fMRI timecourse for each ROI in the network (averaged across ROI voxels), (2) denoised the mean timecourses by removing variability associated with motion parameters, white matter, and CSF signal (i.e., by taking the residuals from linear regression analyses performed on each ROI timecourse with these noise timecourses as regressors), and (3) performed correlation analyses on each pair of ROIs. Motion displacement was estimated during image preprocessing (above), and white matter and ventricle signal were estimated for each subject by extracting the mean signal from four ROIs placed in white matter and lateral ventricles, respectively. For white matter, ROIs were cubes, 343 mm^3 in volume, with center Talairach coordinates (X,Y,Z): ±22, 24, 22 and ±22, 38, 30. For ventricles, ROIs were cubes, 125 mm^3 in volume, with center coordinates (X,Y,Z): ±21, −39, 12; 1, 6, 15; 1, −4, 18. Although many debate the proper procedures for denoising fMRI timecourses for these types of analyses [Hallquist et al., 2013; Power et al., 2012; Satterthwaite et al., 2013], the approach we describe is compatible with current recommendations made by major analysis packages. ROI–ROI connections were calculated using Pearson's r, and transformed to Fisher's Z for subsequent analyses. First, one-sample t-tests identified ROI pairs exhibiting connectivity greater than zero for each group. Then, an ANCOVA (group × mean hearing loss) was performed for each ROI pair to determine whether connectivity differed between groups, and whether RSFC was influenced by hearing loss. Finally, correlations between ROI–ROI relationships and behavioral variables were calculated for tinnitus patients using Pearson's r. We restricted these analyses to three variables to reduce the number of tests performed (and the potential for false positive results): post-MRI tinnitus loudness ratings, THI scores, and GAD scores. We chose post-MRI tinnitus loudness over pre-scan scores in these analyses to reduce the number of tests, and because it was more likely to be representative of patients' experiences during MRI, as it also reflects any effects that scanner noise may have had on tinnitus percepts.

Additional Methodological Considerations Regarding ICA

In ICA, the temporal "concatenative" method is a common way to identify intrinsic functional networks in groups of subjects [Calhoun et al., 2001; Erhardt et al., 2011; Filippini et al., 2009]. In this approach, an initial data-reduction step (using PCA) is performed prior to ICA. Software packages like GIFT (http://icatb.sourceforget.net) or FSL-MELODIC (http://www.fMRIb.ox.ac.uk/fsl/) apply data reduction twice prior to ICA: first to each subject, and then to the concatenated (already reduced) group data [Erhardt et al., 2011]. Subject-level data reduction, in particular, is typically done to reduce computational demands and to aid denoising [Calhoun et al., 2001; Erhardt et al., 2011]. Our approach differed slightly from these, in that Brainvoyager's ICA Plugin performed the initial data-reduction step only once using the entire temporally concatenated dataset, and therefore did not include data reduction on single-subject data. Our data suggest that this latter step is not strictly necessary to identify RSNs.

RESULTS

Demographic, Audiometric, and Behavioral Measures

Patients and controls did not differ in age or sex. Although patients tended to have greater mean hearing loss, loudness discomfort levels, and symptoms of anxiety, these differences were not significant. In patients, tinnitus loudness increased on average, when measured immediately before and after the MRI scan [$t(20) = -4.29$, $P = 0.0004$]; however, not all patients reported increased loudness. Detailed information can be found in Table I.

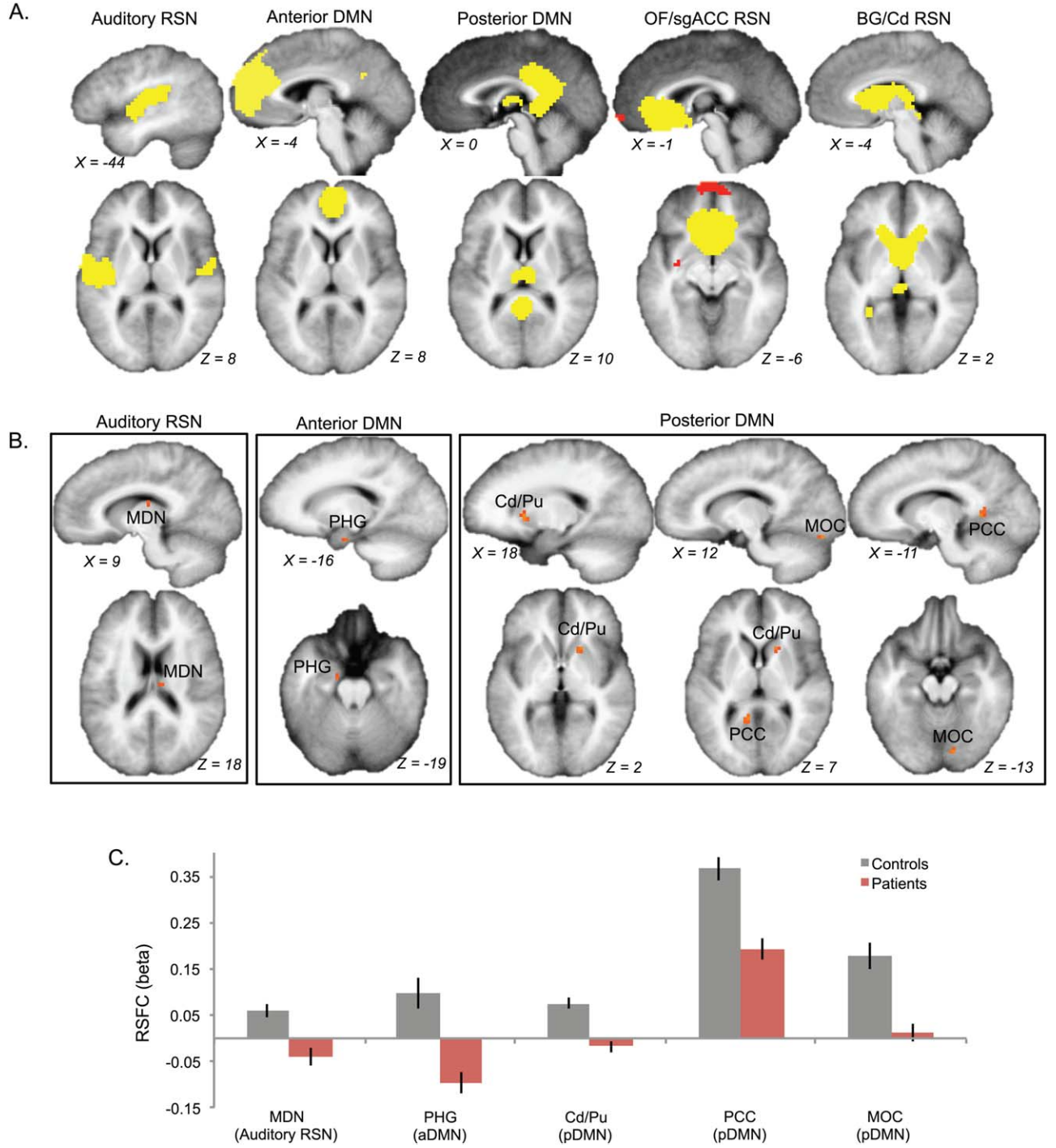

Figure 1.

Comparing typical RSNs in tinnitus patients and controls. (**A**) Five typical RSNs were targeted for statistical analysis between groups (*t*-test; $P_{uncorr} < 0.0005$, $k > 3$), including an auditory–somatomotor RSN, anterior and posterior default-mode networks (DMN), an RSN covering orbitofrontal and subgenual anterior cingulate cortex (OF/sgACC RSN), and a basal ganglia network emphasizing the caudate nucleus (BG/Cd RSN). *Yellow* and *red colors* indicate opposing relationships with each RSN. (**B**) Three RSNs demonstrated statistical differences between groups, and the resulting maps are displayed for each of these RSNs (*orange*). Tinnitus-related reductions in resting-state functional connectivity (RSFC) were noted in the mediodorsal nucleus of the thalamus (MDN), anterior parahippocampal gyrus (PHG), caudate/putamen (Cd/Pu), posterior cingulate cortex (PCC) and medal occipital cortex (MOC). (**C**) RSFC values (beta weights) are plotted for each cluster with respect to its RSN for controls (*gray*) and tinnitus patients (*red*). Error bars indicate standard error of mean. All maps in all figures are displayed on group-averaged anatomical scans in neurological convention (i.e., right hemisphere is located on the right-hand side of the image).

TABLE II. Talairach coordinates of analysis results

Statistical analysis	Region	Talairach center of gravity			Volume (mm^3)
		X	*Y*	*Z*	
Patients vs. controls, RSN: Posterior DMN	Caudate/putamen	15	14	4	297
	Posterior cingulate cortex	−9	−49	7	270
	Medial occipital cortex	−9	−49	7	81
Patients vs. Controls, RSN Anterior DMN	Parahippocampal region	−15	−10	−20	81
Patients vs. Controls, RSN: Auditory	Right mediodorsal nucleus	9	−16	19	81
Tinnitus-only, RSN: Tinnitus Network	Right orbitofrontal cortex	24	38	7	675
	Left orbitofrontal cortex	−24	−50	1	621
	Right rostromedial Heschl's gyrus	42	−16	13	540
	Right mediodorsal nucleus	12	−22	16	432
	Right caudomedial Heschl's gyrus	45	−28	16	405
	Right lateral prefrontal cortex	51	5	31	297
	Left putamen	−21	5	13	270
	Right inferior colliculus	6	−34	−5	189

Abbreviations: RSN, resting-state network; DMN, default-mode network; ICA, independent component analysis.

Comparing Typical RSNs

Five RSNs were targeted for statistical comparisons of RSFC between tinnitus patients and controls due to their overlap with regions implicated in previous tinnitus research, including the auditory system [Gu et al., 2010; Leaver et al., 2011; Melcher et al., 2000, 2009; Seydell-Greenwald et al., 2012, 2014], ventromedial prefrontal and anterior cingulate cortex [Boyen et al., 2013; Leaver et al., 2011, 2012; Seydell-Greenwald et al., 2012], striatum [Cheung and Larson, 2010; Leaver et al., 2011; Maudoux et al., 2012b], thalamus [Mühlau et al., 2006], and posterior cingulate cortex (part of the default mode network with medial prefrontal and anterior cingulate cortex [Maudoux et al., 2012a]). These RSNs were defined using data from both groups, and were spatially similar to typical RSNs identified in previous research [Allen et al., 2011; Damoiseaux et al., 2006; Laird et al., 2011; Smith et al., 2009]. The RSNs were: (1) an "auditory-somatomotor" network including auditory and somatomotor cortices, (2) anterior default-mode network (aDMN), (3) posterior default-mode network (pDMN), (4) a network overlapping orbitofrontal and subgenual anterior cingulate cortex, and (5) a basal-ganglia network centered on the caudate (Fig. 1A).

No group differences were detected at corrected thresholds; however, three RSNs exhibited moderate differences between groups at uncorrected thresholds (single-voxel threshold $P_{uncorr} < 0.0005$, $k > 3$; Fig. 1B,C). In tinnitus patients, clusters in posterior cingulate cortex (PCC), caudate/putamen, and medial occipital cortex were less strongly correlated with posterior DMN as compared with controls. Tinnitus-related reductions in RSFC were also identified between a cluster in the anterior parahippocampal complex and the anterior DMN. In the auditory–somatomotor network, a cluster in the mediodorsal nucleus of the thalamus (also near the pulvinar nucleus) was less strongly correlated with this network in tinnitus patients as compared with controls. Coordinates for all clusters are reported in Table II. In ROI analyses examining the relationships between RSFC in these clusters and tinnitus or behavioral variables [tinnitus loudness scores, tinnitus distress (THI), mean hearing loss, and anxiety (GAD-7)], no significant correlations were found.

Identifying Atypical RSNs

To identify networks that might be present in tinnitus patients and not in controls or vice versa, patterns of RSFC were also analyzed with separate ICAs for tinnitus patients and controls. These analyses identified 15 independent components each in tinnitus patients and control participants where the majority of voxels coincided with gray matter and likely reflected brain networks. Most of these were similar to the typical RSNs previously identified in ICA literature [Allen et al., 2011; Damoiseaux et al., 2006; Laird et al., 2011; Smith et al., 2009], and exhibited spatial similarity between groups (Fig. 2; Supporting Information Figs. S4,S5). Note that some "fracturing" and/or "lumping" of RSNs is expected as demonstrated by previous studies (e.g., the medial prefrontal network is made up of two networks in controls and one network in patients; [Allen et al., 2011; Damoiseaux et al., 2006; Laird et al., 2011; Smith et al., 2009; Uddin et al., 2009]).

One RSN identified with the tinnitus-only ICA was singled out for further analysis due to its low spatial similarity with other RSNs in tinnitus patients or controls (RSN #25 in Fig. 2C; maximum similarity $r = 0.05$; mean similarity $r = 0.007$). Although a second network from the tinnitus-only ICA also exhibited low spatial similarity with other networks (RSN #30 in Fig. 2C; maximum similarity $r = 0.10$; mean similarity $r = 0.0001$), upon visual inspection this second network was similar to a network from

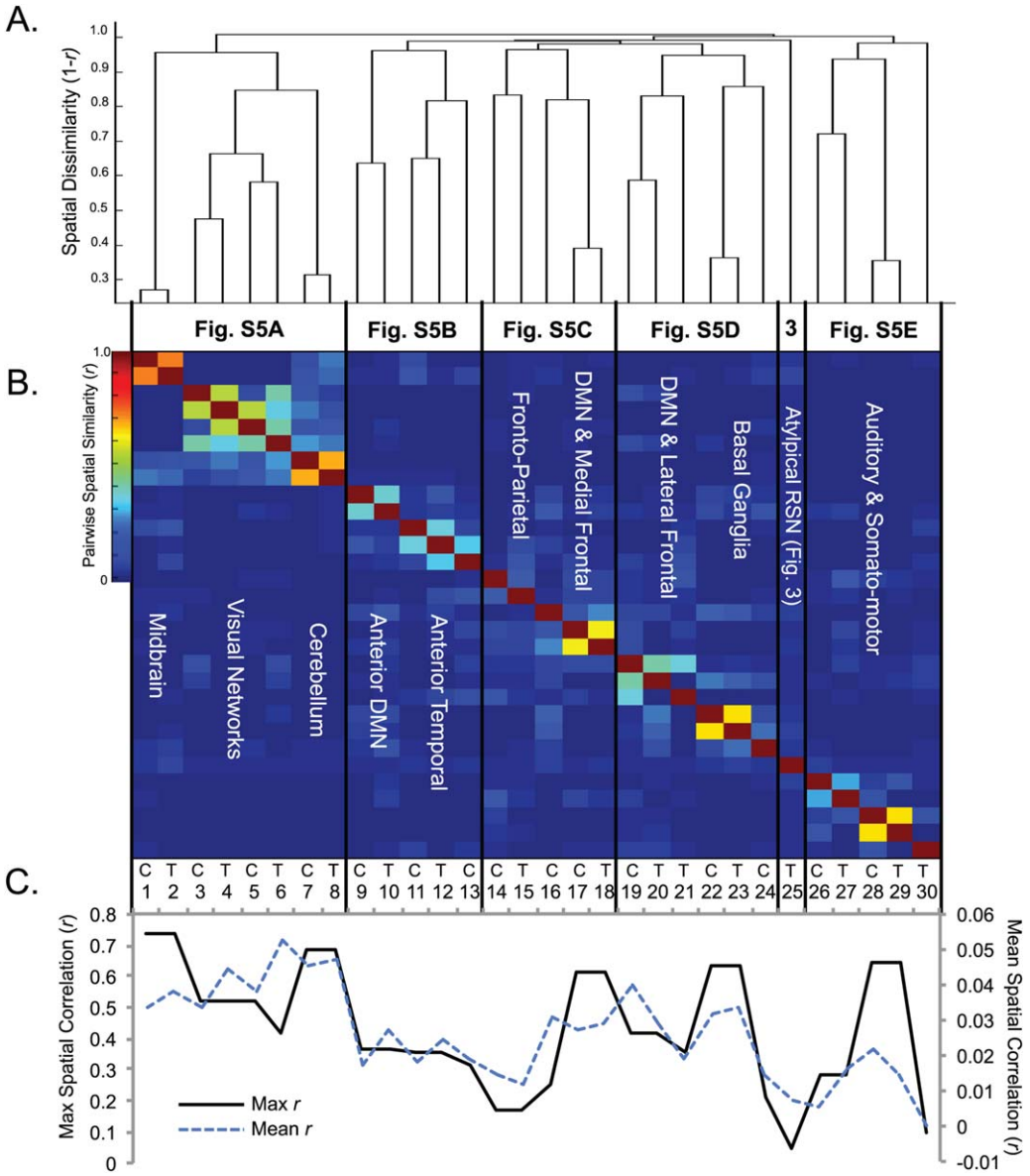

Figure 2.

Spatial similarity of RSNs identified in tinnitus patients and controls. RSNs were analyzed using hierarchical cluster analysis to compare spatial similarity of networks identified using ICA separately for each group. (**A**) A dendrogram of map relationships is plotted, with spatial dissimilarity (1 - Pearson's *r*) on the y axis and node-connections reflecting average Euclidean distance. Each "leaf" node represents an RSN. (**B**) A heatmap of the pairwise spatial cross-correlations between thresholded maps is displayed, with warm colors marking high spatial similarity and cool colors indicating low spatial similarity. The approximate anatomical locations of these networks is described in *white text*. Numbers displayed between panels A and B and *black lines* in B indicate the subsequent Figures in which these maps are shown. (**C**) The maximum or "best" pairwise spatial correlation value is plotted for each map, with respect to all pairwise comparisons made for each map (*black line*, left y-axis). Mean pairwise spatial correlation values are also plotted for each map (*blue dashed* line, right y-axis). Networks with particularly low values would be more likely to be atypical and unique to either tinnitus patients or controls. *Letters* and *numbers* between panels B and C mark group (T, tinnitus patients; C, controls) and RSN index used in Supporting Information Figure S5 for each column, respectively.

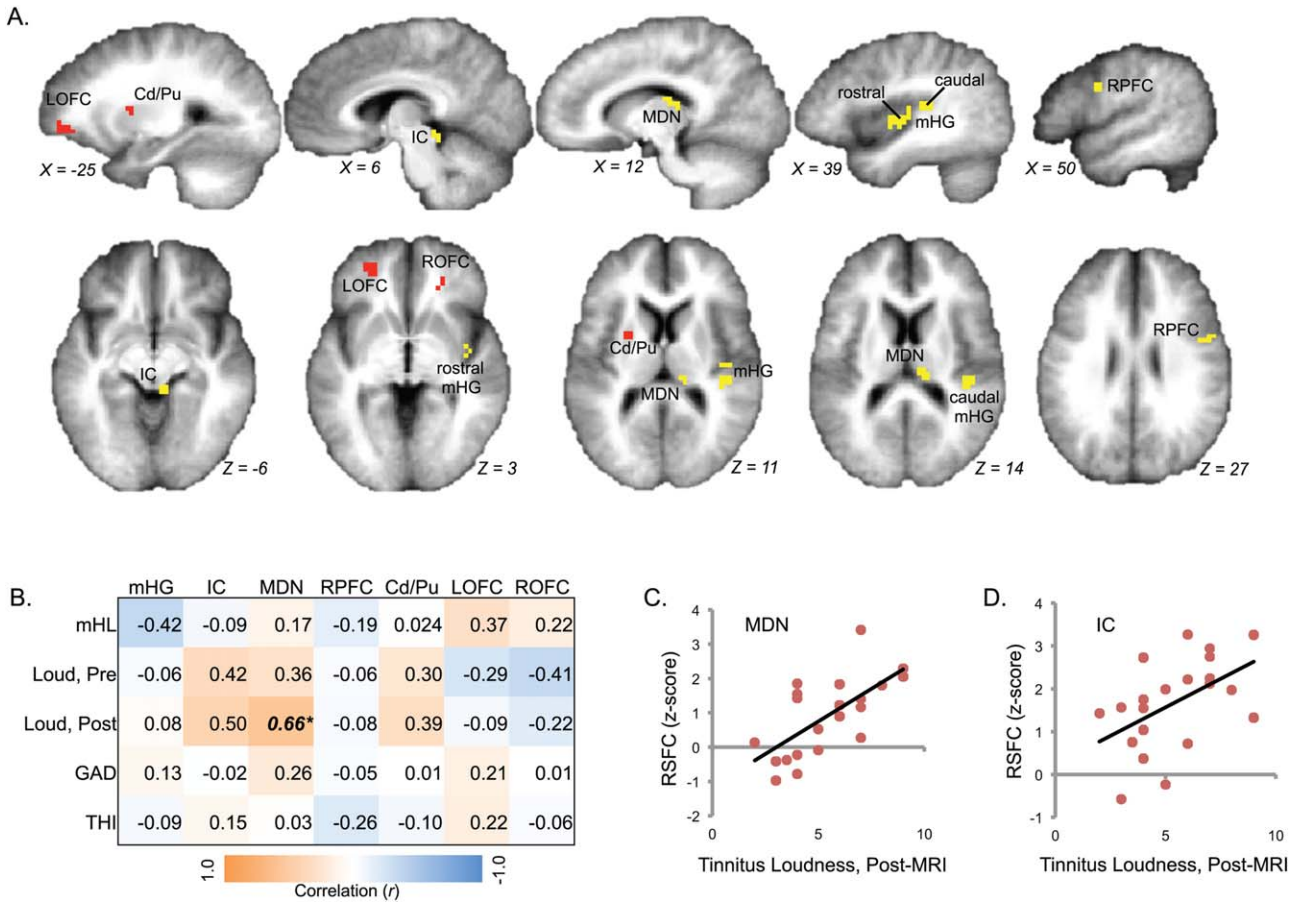

Figure 3.

Atypical RSN in tinnitus patients. (**A**) An RSN was identified in tinnitus patients that was dissimilar to RSNs in controls. This network is displayed on group-averaged anatomy; *red* and *yellow* depict opposing functional relationships (i.e., yellow regions are positively correlated with the RSN-timecourse and red regions are negatively correlated). Clusters overlap with parts of the auditory system, including the inferior colliculus (IC) and two clusters on medial Heschl's gyrus (mHG). Other clusters are located in mediodorsal nucleus of the thalamus (MDN), caudate/putamen (Cd/Pu), right lateral prefrontal cortex (RPFC), and left and right orbitofrontal cortex (LOFC and ROFC). The X and Z Talairach planes are indicated for each slice. (**B**) Correlations between behavioral variables and network-connectivity in these clusters are displayed in a matrix, where orange marks positive correlations and blue marks negative correlations. Significant correlations are indicated in bold and italics ($^*P_{corr} < 0.05$). Effects for caudal and rostral mHG clusters were similar, and were therefore analyzed together in this section (only). (**C, D**) Scatterplots are shown for cases where behavioral variables predict resting-state functional connectivity (RSFC) between clusters and the tinnitus network.

the controls-only ICA (RSN #28, Supporting Information Fig. S5E) and was therefore not targeted for further analysis. The atypical tinnitus RSN is illustrated in Figure 3A. It included the inferior colliculus, medial Heschl's gyrus near primary or "core" auditory cortex, mediodorsal nucleus of the thalamus (also near the pulvinar nucleus), putamen near the caudate nucleus, lateral prefrontal cortex and orbitofrontal cortex. There were two clusters in medial Heschl's gyrus (mHG), one caudal and another rostral extending into the insula (Table II). Two groups of clusters showed opposing relationships to each other in this network: (1) inferior colliculus, caudal and rostral mHG, mediodorsal nucleus, lateral prefrontal cortex and (2) caudate/putamen and bilateral orbitofrontal cortex.

ROI analyses measured the extent to which RSFC within this atypical tinnitus RSN could be explained by behavioral variables. Functional connectivity between the mediodorsal nucleus and this network was strongly correlated with post-MRI ratings of tinnitus loudness ($P_{corr} < 0.05$; Fig. 3B,C). No other correlations met corrected thresholds, although a trend toward a positive correlation with post-MRI loudness was also present in inferior colliculus

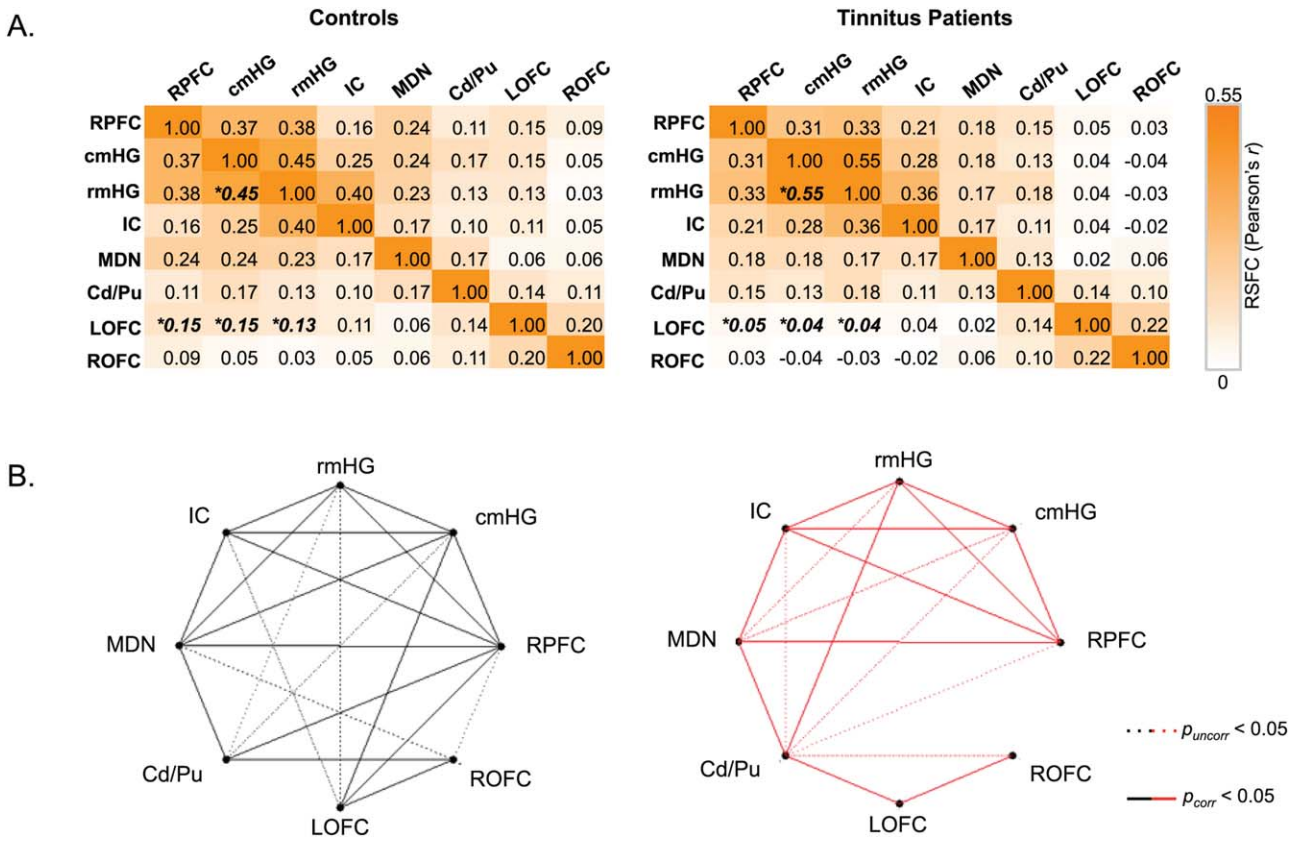

Figure 4.

Exploring the atypical tinnitus RSN. (**A**) Correlations in raw, denoised fMRI signal between regions of the atypical tinnitus RSN are displayed in a cross-correlation matrix, where *deeper orange colors* indicate stronger positive correlations. No regions displayed strong negative correlations in raw signal with any other region of the network. Mean correlation (Pearson's *r*) values are displayed, derived from ROI–ROI analyses performed in single subjects using the clusters from Figure 3A and averaged for healthy controls (left) and in tinnitus patients (right). ROI–ROI relationships that exhibited differences between groups are bolded, italicized, and marked with an *asterisk* ($P_{uncorr} < 0.05$). (**B**) Graphs of the atypical RSN are displayed to highlight the relationships in raw intrinsic fMRI signal between ROIs for controls and patients (at left in *black* and at right in *red*, respectively). *Dotted lines* mark significant correlations at $P_{uncorr} < 0.05$, and *solid lines* mark correlations $P_{corr} < 0.05$, Bonferroni-corrected for the number of pairwise tests.

($r = 0.50$, $P_{uncorr} = 0.02$; Fig. 3D). Thus, activity in mediodorsal nucleus and, to a lesser extent, inferior colliculus, was more correlated with this network in patients experiencing louder tinnitus after the MRI scan.

Exploratory Analyses of an Atypical RSN

In contrast to the analyses described above that measured ICA-defined RSFC within RSNs, this exploratory analysis measured region-to-region (vs. region-to-RSN) correlations in fMRI activity amongst the ROIs of the atypical tinnitus RSN. In this analysis, resting-state fMRI activity was positively correlated in many ROI–ROI pairs for both tinnitus patients and controls (Fig. 4), and many more ROI–ROI pairs showed significant positive correlations in fMRI signal in controls than in tinnitus patients. No regions displayed strong negative correlations in raw signal with other regions in the network. Regions exhibiting the strongest intercorrelations followed a similar pattern to the opposing relationships of the atypical tinnitus RSN (i.e., Fig. 3) in both tinnitus patients and controls, and roughly formed two groups: (1) auditory ROIs, mediodorsal nucleus, and prefrontal cortex were intercorrelated and (2) caudate/putamen and orbitofrontal ROIs were also intercorrelated.

To determine whether ROI-ROI connections differed between groups or were affected by hearing loss, we

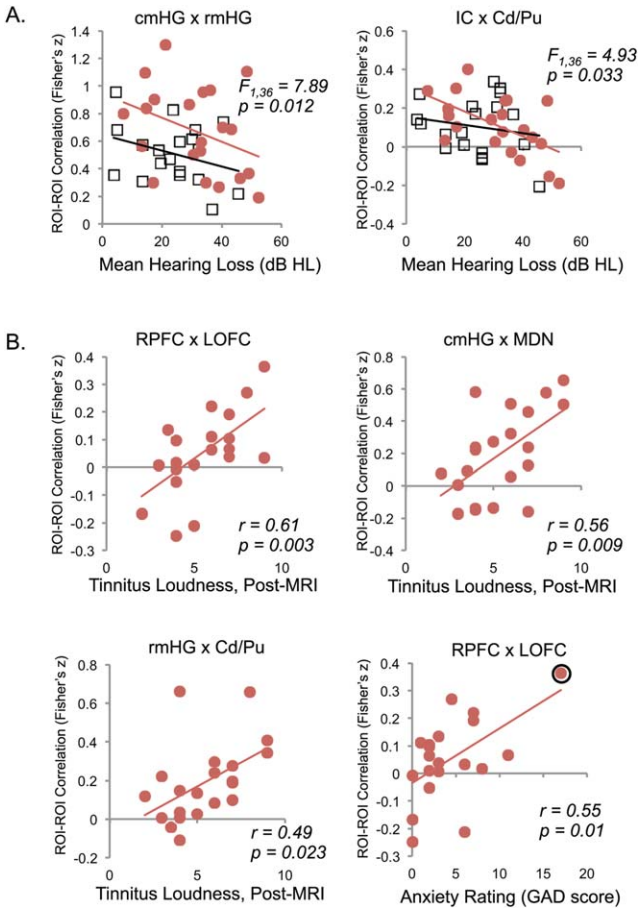

Figure 5.

Relationships between hearing loss, tinnitus variables, and raw intrinsic connectivity in the atypical tinnitus RSN. (**A**) Significant correlations between mean hearing loss (mHL) and ROI–ROI correlations in raw fMRI signal across both groups were identified using a Group × mHL ANCOVA. Scatterplots of ROI pairs exhibiting significant ($P_{uncorr} < 0.05$) effects of mHL are displayed. Patient data are shown in *red circles*, and controls in *black squares*. (**B**) Scatterplots are shown for ROI pairs demonstrating significant correlations between behavioral variables (i.e., post-MRI tinnitus loudness ratings and anxiety rating scale scores) and ROI–ROI raw intrinsic connectivity ($P_{uncorr} < 0.05$) as assessed in tinnitus patients using Pearson's *r*. A potential outlier is encircled in the lower right panel; statistics with this datapoint omitted are $r = 0.35$, $P = 0.14$.

performed an ANCOVA (group × mean hearing loss) for each pair of ROIs (Supporting Information Table S1). No effects survived corrected thresholds. However, four ROI-ROI connections demonstrated moderate differences between groups (Fig. 4). Functional connectivity between the caudal and rostral mHG ROIs was stronger in tinnitus patients than in controls ($F(1,36) = 6.29$, $P = 0.01$; c.f. [Seydell-Greenwald et al., 2014]). Also, connections between the left orbitofrontal cortex (LOFC) and (1) right lateral prefrontal cortex (RPFC), (2) caudal mHG, and (3) rostral mHG were stronger in controls than in tinnitus patients [$F(1,36) = 8.20$, $P = 0.007$; $F(1,36) = 11.74$, $P = 0.002$; and $F(1,36) = 5.90$, $P = 0.02$, respectively].

Functional connections between two ROI–ROI pairs were also affected by mean hearing loss ($P < 0.05$, Fig. 5A), with connectivity between auditory cortex ROIs (caudal and rostral mHG) and between the right inferior colliculus and caudate/putamen negatively correlated with mean hearing loss [$F(1,36) = 7.89$, $P = 0.012$ and $F(1,36) = 4.93$, $P = 0.033$, respectively]. No interactions between group and hearing loss were significant, although some trends were present (e.g., between subcortical auditory ROIs and caudal mHG; Supporting Information Table S1).

We also examined relationships between ROI–ROI correlations and (1) post-MRI tinnitus loudness, (2) tinnitus distress (THI score), and (3) symptoms of anxiety (GAD score) in tinnitus patients. No tests survived corrected thresholds. However, moderate positive correlations were present between post-MRI tinnitus loudness and three ROI-ROI pairs (Fig. 5B): caudal mHG and mediodorsal nucleus ($r = 0.56$, $P = 0.009$), RPFC and LOFC ($r = 0.61$, $P = 0.003$), and rostral mHG and Cd/Pu ($r = 0.49$, $P = 0.023$). A positive relationship was also present between anxiety and RPFC–LOFC connectivity; however, this effect may have been influenced by an outlier (Fig. 5B).

DISCUSSION

In this study, we demonstrated tinnitus-related differences in RSFC for both typical and atypical RSNs, including auditory and non-auditory regions previously implicated in tinnitus pathophysiology [Cheung and Larson, 2010; Landgrebe et al., 2009; Leaver et al., 2011; Maudoux et al., 2012a,b; Vanneste et al., 2010]. Some of these regions, like the mediodorsal nucleus of the thalamus and striatum (caudate/putamen), demonstrated tinnitus-related effects in both typical and atypical RSNs. When defining RSNs separately in patients, we identified an atypical RSN that engaged medial Heschl's gyrus, inferior colliculus, mediodorsal nucleus, striatum, orbitofrontal cortex, and lateral prefrontal cortex. The network's presence in the tinnitus-only ICA suggests that connectivity within this network explained a greater and/or unique amount of variance in patients than in controls, and may reflect the neural circuitry underlying tinnitus. Indeed, connectivity in the mediodorsal nucleus was positively correlated with tinnitus loudness reported after the MRI scan, perhaps indicating its role in the auditory–sensory experience of tinnitus. Taken together, our results suggest that unique functional relationships exist between auditory and non-auditory regions in people with tinnitus, and point to an auditory and thalamo-striato-frontal circuit involved in tinnitus pathophysiology [Rauschecker et al., 2010].

The Role of Typical RSNs in Understanding Tinnitus Pathophysiology

Functional connectivity methods in fMRI are still relatively new, and optimal analysis strategies are under development [Fox and Greicius, 2010; Van Essen et al., 2012; Wig et al., 2014]. Defining typical RSNs using ICA is an asset, in that it allows us to probe functional connectivity in well characterized, large-scale networks that have been previously studied in other contexts and disorders [Allen et al., 2011; Baliki et al., 2008; Damoiseaux et al., 2006; Greicius et al., 2004, 2007; Laird et al., 2011; Leaver et al., 2015a; Smith et al., 2009]. Furthermore, this approach permits examination of functional relationships within a given RSN independent of other RSNs (i.e., with temporal variability in brain activity attributable to other RSNs statistically removed), which may capture different aspects of RSFC than seed-region or ROI analyses. However, it is unlikely that any one typical RSN will capture the entirety of a given pathology; in our case, tinnitus is unlikely to be solely explained by dysfunction in the auditory RSN or DMN. Rather, we use typical RSNs to indirectly probe regions we consider to be relevant to tinnitus [Davies et al., 2014; Maudoux et al., 2012a,b], while hypothesizing that tinnitus and other disorders involve network-level dysfunction that exists outside of typical RSNs.

In the present study, we chose five typical RSNs [Allen et al., 2011; Damoiseaux et al., 2006; Laird et al., 2011; Smith et al., 2009] to probe function in structures thought to be critical for tinnitus. We saw tinnitus-related reductions in connectivity between the posterior default-mode network and the striatum, posterior cingulate cortex (PCC), and medial occipital cortex. We also noted tinnitus-related reductions in connectivity between the mediodorsal nucleus and an auditory RSN, and between the left anterior parahippocampal gyrus (PHG) and the anterior DMN. Our findings support previous reports of tinnitus-related differences in these regions (i.e., basal ganglia [Cheung and Larson, 2010; Leaver et al., 2011; Maudoux et al., 2012b], PCC [Maudoux et al., 2012a; Vanneste et al., 2010], thalamus [Mühlau et al., 2006], PHG [Landgrebe et al., 2009; Maudoux et al., 2012a; Vanneste et al., 2011a]), specifically including reduced connectivity between PCC and DMN in tinnitus [Schmidt et al., 2013]. However, although functional connectivity in these regions was different in tinnitus patients, none of these effects were correlated with tinnitus or other behavioral variables. PCC and PHG have been previously associated with measures of tinnitus distress [Maudoux et al., 2012a; Vanneste et al., 2010]; perhaps the relatively limited range of distress/THI scores in the current study was not conducive to detecting these effects.

Reduced functional connectivity between these regions and their respective RSNs could be explained in multiple ways, which are not mutually exclusive. These regions could be underperforming due to reductions in neuronal tissue or synapses, resulting in reduced functional output. This is a typical interpretation of clinical neuroimaging research using RSNs to probe for aberrant function [Baliki et al., 2008; Greicius et al., 2004]. Indeed, previous studies have demonstrated tinnitus-related anatomical anomalies in the thalamus [Mühlau et al., 2006; Seydell-Greenwald et al., 2014], inferior colliculus and auditory cortex [Seydell-Greenwald et al., 2014], and parahippocampal regions [Landgrebe et al., 2009], which could explain abnormal function in these structures reported in the current study. It is also possible that effects identified by ICA in typical and atypical RSNs reflect other signals present in the tinnitus data that are unrelated to brain organization underlying tinnitus. Yet another alternative interpretation is that these regions have normal functional capabilities, but are not connected in a temporally coherent manner to the typical RSN of interest. Certainly, cases of overlap between results of the "typical RSN" analysis (Fig. 1) and the "atypical tinnitus RSN" (Fig. 3) could support this interpretation. For example, perhaps the mediodorsal nucleus was less functionally connected with the auditory RSN in patients than controls because it was more connected with the tinnitus RSN or other atypical RSNs. Analysis methods that are able to directly identify and measure "atypical" networks relevant for tinnitus or other disorders without making assumptions *a priori* regarding regions of interest are needed. We believe that our tinnitus-only ICA identified such a "tinnitus network" in this way, but more work is needed to develop methodological approaches identifying disorder-specific (rather than typical) RSNs if we hope to achieve a complete understanding of tinnitus and other brain-network disorders.

Atypical RSNs and a Possible Tinnitus Network

To our knowledge, no previous ICA study of resting-state fMRI has identified atypical RSNs relevant to the pathophysiology of a clinical sample; by contrast, EEG studies do have a history of characterizing atypical networks using ICA and similar blind source separation analyses, including tinnitus research [De Ridder et al., 2011b; Vanneste et al., 2014]. In the current study, we identified a network that was uniquely present in tinnitus patients in our analyses, including both auditory regions (medial Heschl's gyrus, inferior colliculus) and fronto-striatal regions (mediodorsal nucleus, striatum, lateral prefrontal cortex, and orbitofrontal cortex). In a secondary analysis we confirmed that this "tinnitus network" was functionally connected in controls, suggesting that functional connectivity between regions of this network is neurophysiologically plausible. However, two differences were apparent: (1) auditory regions were not functionally connected with non-auditory regions in patients (i.e., their timecourses were not positively correlated) and (2) connectivity within the atypical tinnitus RSN explained a greater amount of the overall variance in fMRI timecourses across patients' brains than controls' brains

(hence its presence in the tinnitus-only ICA; see also Supporting Information Fig. S5).

Tinnitus is relatively unique as an object of study with resting-state fMRI, in that these patients constantly experience a sensory perception not experienced by controls. Thus, it is possible that connectivity within this tinnitus network could reflect the tinnitus percept itself, and that the regions constituting this network may be responsible for generating, perpetuating, and/or reacting to the tinnitus percept. Indeed, functional connectivity between some regions in this network was positively correlated with the loudness of tinnitus reported after the MRI scan. The mediodorsal nucleus, and to a lesser extent the inferior colliculus, were more connected with the tinnitus network in patients with louder tinnitus. Furthermore, correlations between fMRI timecourses in the mediodorsal nucleus and caudal mHG were also positively correlated with tinnitus loudness, as assessed in ROI-ROI analyses *post hoc*; correlations between the inferior colliculus and striatum were also positively correlated with tinnitus loudness in this analysis. The caudal mHG is likely to be either core (primary) or medial belt (secondary) auditory cortex, and its neurons likely respond to simple, tone- or noise-like stimuli typical of tinnitus sensations [Kaas and Hackett, 2000; Kusmierek and Rauschecker, 2014; Rauschecker et al., 1995]. The latter is also true of the inferior colliculus (a brainstem structure of the ascending auditory–sensory pathway). The mediodorsal nucleus is connected with both fronto-limbic [Behrens et al., 2003; Goldman-Rakic and Porrino, 1985; McDonald, 1987; Ray and Price, 1993] and auditory regions [Pandya et al., 1994; Tanibuchi and Goldman-Rakic, 2003]. This cluster may have also overlapped with the pulvinar, a multisensory nucleus connected with the auditory system [Huang and Lindsley, 1973; de la Mothe et al., 2012; Romanski et al., 1997]. Connectivity within these structures could be responsible for the auditory-sensory experience of tinnitus, while dysfunction in these and other members of the tinnitus network may reflect tinnitus chronicity and/or reactions to tinnitus.

Indeed, in the context of ICA, we report an opposing functional relationship in the tinnitus network between auditory–sensory regions (plus right lateral PFC) and fronto-striatal regions, including caudate/putamen and orbitofrontal cortex. In other words, intrinsic activity in auditory–sensory and lateral PFC regions was negatively correlated with intrinsic activity in medial fronto-striatal regions when temporal variance associated with other RSNs (e.g., auditory network) was statistically removed. This suggests that activity in the auditory and medial fronto-striatal parts of the tinnitus network may influence each other indirectly and/or directly. As has been previously suggested [Rauschecker et al., 2010, 2015], fronto-striatal regions may receive tinnitus-related input from the auditory system through the thalamus, and in response attempt (unsuccessfully) to attenuate the unwanted, irrelevant tinnitus percept. However, causal relationships between activity in these regions and the development of chronic tinnitus remain to be tested.

Correlations in fMRI timecourses between right lateral prefrontal and left orbitofrontal ROIs were positively correlated with post-MRI tinnitus loudness. The relationship between lateral frontal connectivity and tinnitus loudness more likely reflects increased attentional demands and/or unsuccessful attempts to ignore or attenuate the tinnitus during the resting-state scan, rather than the sensory perception of tinnitus. Our previous work has demonstrated that lateral prefrontal activity during an auditory oddball task was also positively correlated with post-MRI tinnitus loudness ratings [Seydell-Greenwald et al., 2012]. This is in contrast to medial fronto-striatal dysfunction, which we have argued is critical to the sensory perception of tinnitus. Although some frontal and auditory ROIs were right-lateralized, we do not make strong claims regarding the significance of this lateralization, especially considering that the great majority of patients in the current study experience bilateral tinnitus.

Because our findings were novel for resting-state fMRI, we used several measures to probe the legitimacy of the tinnitus network. First, we confirmed the presence of the network over multiple iterations of ICA (see "Materials and Methods" section); it was present in 10 of 10 ICA repetitions on patients' fMRI data. In control data, no network (also examined with visual inspection) was identified that was spatially similar to the tinnitus network at our chosen parameters and thresholds (Fig. 2; Supporting Information Fig. S5). Second, we performed exploratory ROI-ROI analyses to confirm connectivity within the tinnitus network in both patients and controls (and thus its neurobiological validity). These ROI–ROI analyses demonstrated that network regions were functionally connected in both groups, with a greater number of positively correlated ROI pairs in controls. (Although the lack of negative correlation between these regions in the ROI–ROI analysis may appear contradictory, the ROI–ROI analysis does not remove temporal signal associated with other RSNs like ICA.) Taken together, these two probes suggest that, although activity in "tinnitus network" regions was functionally correlated in controls (as evident in the ROI–ROI analysis), connectivity within this "tinnitus network" does not explain a large amount of overall variance in control data (as evident from its absence in the controls-only ICA with our chosen parameters). In addition, our analyses addressed potential contamination of the tinnitus network by noise, by removing sources of nuisance variability (i.e., motion, physiological noise captured by white-matter and cerebrospinal-fluid signal) from ROI timecourses prior to exploratory ROI–ROI analyses of the tinnitus network in both groups of volunteers. Similarly, because ICA successfully identifies separate components related to motion, physiological, and other sources of noise [Perlbarg et al., 2007; Thomas et al., 2002], it is unlikely that those sources of noise influenced the definition of the tinnitus network

with ICA. We also examined the power spectra of all RSN timecourses, and the atypical tinnitus RSN was not appreciably different from other networks in this respect (Supporting Information Fig. S6). The tinnitus network was robust to the probes we selected, and so we are quite confident that the network is neurophysiologically plausible. Moreover, RSFC in parts of this network was correlated with post-scan tinnitus-loudness ratings, which further enhances our confidence that the network is related to tinnitus (rather than emerging from spurious differences between groups).

Additional Methodological Considerations

As with all research, study results are necessarily constrained by the methodological approach chosen. In our study, we used ICA to analyze resting brain activity and to make inferences regarding the functional "connections" between brain regions. Although we have discussed the limitations of this technique throughout the article, some additional methodological considerations may be worth noting here. For example, our analyses targeted a limited sample of RSNs to reduce Type I error, which may have caused us to miss tinnitus-related effects in networks not assessed (e.g., in the hippocampus or cerebellum). It is also possible that we missed effects in superior parietal or occipital cortex due to the positioning of our functional EPIs, which we did to boost signal-to-noise in ventral prefrontal cortex. In addition, we did not measure temporal dependencies between brain activity within the tinnitus network or other networks. Future studies measuring brain activity with greater temporal resolution and with a larger field of view will be in a better position to infer causal relationships between activity in these and other brain networks. We also reported some results that did not survive our strict corrected thresholds, which means that validation of these results in an independent patient cohort, and perhaps using different, yet complementary, methodological approaches, is needed.

Tinnitus has long been associated with hearing difficulties [Hoffman and Reed, 2004], and ruling out hearing loss as an alternative explanation for any observed effects is always an important methodological consideration in tinnitus research. In our sample, mean hearing levels were not different between groups, though a trend was present for greater loss in patients. Nevertheless, differences in hearing loss seemed not to contribute to our between-groups effects, as no correlations were found with hearing thresholds in regions exhibiting tinnitus-related effects. It is possible that our groups differed in the etiology of their hearing loss, which may have had different neurobiological consequences [Melcher et al., 2012]. We did note a modest negative correlation between mean hearing levels and functional connectivity between auditory cortex ROIs in the tinnitus network for both patients and controls, supporting our previous report of reduced white-matter integrity with hearing loss [Seydell-Greenwald et al., 2014]. Deafferentation could have reduced temporally coherent intrinsic activity in the auditory cortex; typical models predict increased spontaneous activity, at least initially [Eggermont and Roberts, 2004]. Negative relationships between hearing loss and functional connectivity in other structures like frontal cortex could reflect compensatory strategies or more widespread effects of deafferentation [Pawela et al., 2010] and/or reduced hearing thresholds. Note too that hearing levels were highly correlated with age in the current study ($r = 0.71$ for patients, $r = 0.86$ for controls), as is to be expected [Hoffman and Reed, 2004]. A thorough look at hearing loss is outside the scope of this study, and more work is sorely needed in this underrepresented area of neuroimaging research. We are reasonably confident, however, that hearing loss is not driving the tinnitus-related effects reported in the current study.

Tinnitus patients and controls did not differ in anxiety (or depression) scores, and we found no relationships between functional connectivity measures and tinnitus-related distress or sub-clinical symptoms of anxiety (or depression) in the current study. We did, however, observe tinnitus-related differences in functional connectivity in regions that are considered limbic by virtue of their connections with anterior- and medial-temporal structures associated with emotion, including some regions previously associated with tinnitus-related distress [i.e., PCC and PHG; Maudoux et al., 2012a; Vanneste et al., 2010]. It is certainly possible that these and other limbic structures are engaged in patients experiencing distress or anxiety relating to their tinnitus [Leaver et al., 2012; Vanneste et al., 2010]. Both the ventral striatum and orbito-/pre-frontal cortices are engaged when experiencing aversive (and pleasant) stimuli [Jensen et al., 2003; Plassmann et al., 2010; Roitman et al., 2005; Wager et al., 2008]; therefore, the effects that we observed in these structures may have been related to unpleasantness associated with tinnitus. It is also possible that functional connectivity as measured by fMRI is not affected by tinnitus distress in these regions, while other measures are affected, like EEG/MEG measures of higher frequency connectivity and activity, or anatomical variables. Controversy exists regarding the exact role that distress and emotions play in tinnitus pathophysiology. Some theories propose that emotional responses are critical, or even necessary, in transitioning from acute to chronic tinnitus [Jastreboff, 1990; De Ridder et al., 2011a]. Others have proposed that, while stress and negative emotions can exacerbate tinnitus, these reactions are not necessary for tinnitus to become chronic [Leaver et al., 2011, 2012; Rauschecker et al., 2010]. Indeed, there is evidence for separation in the neural systems subserving the auditory-sensory experience of tinnitus from those supporting tinnitus-related distress [Leaver et al., 2012; Vanneste et al., 2014]. Patients in our study had a relatively wide range of tinnitus distress scores, but were overall on the low-to-moderate end of the spectrum; only

one patient met the criteria for moderate distress (58–76 THI score) and one patient had a severe score (78–100), while others fell in the slight and mild impact categories [Newman et al., 1996]. Future research designed to directly address the role of distress and mental health in tinnitus and other similar sensory disorders like chronic pain are needed, perhaps through directed recruiting of patients with severe distress and/or comorbid mood disorders [Joos et al., 2012].

CONCLUSIONS

Studies using functional neuroimaging to record brain activity directly related to tinnitus in humans have been faced with several challenges. Research using task-fMRI has used stimulus-evoked activity to make indirect inferences regarding tinnitus-related activity [Gu et al., 2010; Leaver et al., 2011; Melcher et al., 2009], and although resting-state fMRI studies may be in a better position to directly measure activity associated with tinnitus (rather than an experimentally generated stimulus), they have so far relied on assumptions made *a priori* regarding the critical regions of interest (for seed-based analyses) or the key large-scale, typical RSNs of interest (for ICA studies). EEG and MEG research is more likely to use blind source-separation techniques to identify unique networks relevant for tinnitus [e.g., Vanneste et al., 2014]; however, some rely on the same prior assumptions made in fMRI studies and coarse spatial resolution is a concern. Here, we present a "tinnitus network" uniquely present in tinnitus patients, identified without restrictions made *a priori* and checked for validity by several assessments. This is the first time, to our knowledge, that a unique, atypical network has been identified for a brain disorder using ICA of resting-state fMRI in this way, and our results support previous tinnitus research [Leaver et al., 2011, 2012; Mühlau et al., 2006; Seydell-Greenwald et al., 2012, 2014], and theoretical models [Leaver et al., 2015b; Rauschecker et al., 2010, 2015], suggesting that tinnitus pathophysiology involves crosstalk, and perhaps dysregulation, between fronto-striatal and auditory–sensory regions. Nevertheless, much more work is needed to determine causal relationships in the function of these regions as they relate to chronic tinnitus, as well as the impact of hearing loss, aging, tinnitus-related distress, and other factors on tinnitus pathophysiology. Brain connectivity research shows great promise in its ability to enrich our understanding of this network disorder, and we hope this leads to more effective treatments and perhaps a cure for tinnitus.

ACKNOWLEDGMENT

We wish to thank Sylke-Monina Chowdhury for her technical assistance.

REFERENCES

Allen EA, Erhardt EB, Damaraju E, Gruner W, Segall JM, Silva RF, Havlicek M, Rachakonda S, Fries J, Kalyanam R, Michael AM, Caprihan A, Turner JA, Eichele T, Adelsheim S, Bryan AD, Bustillo J, Clark VP, Feldstein Ewing SW, Filbey F, Ford CC, Hutchison K, Jung RE, Kiehl KA, Kodituwakku P, Komesu YM, Mayer AR, Pearlson GD, Phillips JP, Sadek JR, Stevens M, Teuscher U, Thoma RJ, Calhoun VD (2011): A baseline for the multivariate comparison of resting-state networks. Front Syst Neurosci 5:2.

Baliki MN, Geha PY, Apkarian a. V, Chialvo DR (2008): Beyond feeling: Chronic pain hurts the brain, disrupting the default-mode network dynamics. J Neurosci 28:1398–1403.

Behrens TEJ, Johansen-Berg H, Woolrich MW, Smith SM, Wheeler-Kingshott CAM, Boulby PA, Barker GJ, Sillery EL, Sheehan K, Ciccarelli O, Thompson AJ, Brady JM, Matthews PM (2003): Non-invasive mapping of connections between human thalamus and cortex using diffusion imaging. Nat Neurosci 6:750–757.

Boyen K, Langers DRM, de Kleine E, van Dijk P (2013): Gray matter in the brain: Differences associated with tinnitus and hearing loss. Hear Res 295:67–76.

Burton H, Wineland A, Bhattacharya M, Nicklaus J, Garcia KS, Piccirillo JF (2012): Altered networks in bothersome tinnitus: A functional connectivity study. BMC Neurosci 13:3.

Calhoun VD, Adali T, Pearlson GD, Pekar JJ (2001): A method for making group inferences from functional MRI data using independent component analysis. Hum Brain Mapp 14:140–151.

Cheung SW, Larson PS (2010): Tinnitus modulation by deep brain stimulation in locus of caudate neurons (area LC). Neuroscience 169:1768–1778.

Damoiseaux JS, Rombouts SARB, Barkhof F, Scheltens P, Stam CJ, Smith SM, Beckmann CF (2006): Consistent resting-state networks across healthy subjects. Proc Natl Acad Sci USA 103: 13848–13853.

Damoiseaux JS, Prater KE, Miller BL, Greicius MD (2012): Functional connectivity tracks clinical deterioration in Alzheimer's disease. Neurobiol Aging 33:828.e19–830.e19.

Davies J, Gander PE, Andrews M, Hall DA (2014): Auditory network connectivity in tinnitus patients: A resting-state fMRI study. Int J Audiol 53:192–198.

de la Mothe LA, Blumell S, Kajikawa Y, Hackett TA (2012): Thalamic connections of auditory cortex in marmoset monkeys: Lateral belt and parabelt regions. Anat Rec 295:822–836.

De Ridder D, Elgoyhen AB, Romo R, Langguth B (2011a): Phantom percepts: Tinnitus and pain as persisting aversive memory networks. Proc Natl Acad Sci USA 108:8075–8080.

De Ridder D, Vanneste S, Congedo M (2011b): The distressed brain: A group blind source separation analysis on tinnitus. PLoS One 6:e24273.

Deichmann R, Gottfried JA, Hutton C, Turner R (2003): Optimized EPI for fMRI studies of the orbitofrontal cortex. Neuroimage 19:430–441.

Eggermont JJ, Roberts LE (2004): The neuroscience of tinnitus. Trends Neurosci 27:676–682.

Eichhammer P, Hajak G, Kleinjung T, Landgrebe M, Langguth B (2007): Functional imaging of chronic tinnitus: The use of positron emission tomography. Prog Brain Res 166:83–88.

Engineer ND, Riley JR, Seale JD, Vrana WA, Shetake JA, Sudanagunta SP, Borland MS, Kilgard MP (2011): Reversing

pathological neural activity using targeted plasticity. Nature 470:101–104.
Erhardt EB, Rachakonda S, Bedrick EJ, Allen EA, Adali T, Calhoun VD (2011): Comparison of multi-subject ICA methods for analysis of fMRI data. Hum Brain Mapp 32:2075–2095.
Filippini N, MacIntosh BJ, Hough MG, Goodwin GM, Frisoni GB, Smith SM, Matthews PM, Beckmann CF, Mackay CE (2009): Distinct patterns of brain activity in young carriers of the APOE-epsilon4 allele. Proc Natl Acad Sci USA 106:7209–7214.
Formisano E, Esposito F, Di Salle F, Goebel R (2004): Cortex-based independent component analysis of fMRI time series. Magn Reson Imaging 22:1493–1504.
Fox MD, Greicius M (2010): Clinical applications of resting state functional connectivity. Front Syst Neurosci 4:19.
Goldman-Rakic PS, Porrino LJ (1985): The primate mediodorsal (MD) nucleus and its projection to the frontal lobe. J Comp Neurol 242:535–560.
Greicius MD, Srivastava G, Reiss AL, Menon V (2004): Default-mode network activity distinguishes Alzheimer's disease from healthy aging: Evidence from functional MRI. Proc Natl Acad Sci USA 101:4637–4642.
Greicius MD, Flores BH, Menon V, Glover GH, Solvason HB, Kenna H, Reiss AL, Schatzberg AF (2007): Resting-state functional connectivity in major depression: Abnormally increased contributions from subgenual cingulate cortex and thalamus. Biol Psychiatry 62:429–437.
Gu JW, Halpin CF, Nam EC, Levine RA, Melcher JR (2010): Tinnitus, diminished sound-level tolerance, and elevated auditory activity in humans with clinically normal hearing sensitivity. J Neurophysiol 104:3361–3370.
Hallquist MN, Hwang K, Luna B (2013): The nuisance of nuisance regression: Spectral misspecification in a common approach to resting-state fMRI preprocessing reintroduces noise and obscures functional connectivity. Neuroimage 82:208–225.
Henry JA, Dennis KC, Schechter MA (2005): General review of tinnitus: Prevalence, mechanisms, effects, and management. J Speech Lang Hear Res 48:1204–1235.
Hoffman HJ, Reed GW (2004): Epidemiology of tinnitus. In: Snow, JB, editor. Tinnitus: Theory and Management. Hamilton, Ont.: BC Decker, Inc.
Huang CC, Lindsley DB (1973): Polysensory responses and sensory interaction in pulvinar and related postero-lateral thalamic nuclei in cat. Electroencephalogr Clin Neurophysiol 34: 265–280.
Husain FT, Schmidt SA (2014): Using resting state functional connectivity to unravel networks of tinnitus. Hear Res 307: 153–162.
Hyvarinen A (1999): Fast ICA for noisy data using Gaussian moments. In:. ISCAS'99. Proceedings of the 1999 IEEE International Symposium on Circuits and Systems VLSI (Cat. No.99CH36349), Vol. 5. Orlando, FL. pp 57–61.
Jastreboff PJ (1990): Phantom auditory perception (tinnitus): Mechanisms of generation and perception. Neurosci Res 8:221–254.
Jensen J, McIntosh AR, Crawley AP, Mikulis DJ, Remington G, Kapur S (2003): Direct activation of the ventral striatum in anticipation of aversive stimuli. Neuron 40:1251–1257.
Joos K, Vanneste S, De Ridder D (2012): Disentangling depression and distress networks in the tinnitus brain. Ed. Berthold Langguth. PLoS One 7:e40544.
Kaas JH, Hackett TA (2000): Subdivisions of auditory cortex and processing streams in primates. Proc Natl Acad Sci USA 97: 11793–11799.
Kim J, Kim Y, Lee S, Seo J-H, Song H-J, Cho JH, Chang Y (2012): Alteration of functional connectivity in tinnitus brain revealed by resting-state fMRI?: A pilot study. Int J Audiol 51:413–417.
Kusmierek P, Rauschecker JP (2014): Selectivity for space and time in early areas of the auditory dorsal stream in the rhesus monkey. J Neurophysiol 111:1671–1685.
Laird AR, Fox PM, Eickhoff SB, Turner JA, Ray KL, McKay DR, Glahn DC, Beckmann CF, Smith SM, Fox PT (2011): Behavioral interpretations of intrinsic connectivity networks. J Cogn Neurosci 23:4022–4037.
Landgrebe M, Langguth B, Rosengarth K, Braun S, Koch A, Kleinjung T, May A, de Ridder D, Hajak G (2009): Structural brain changes in tinnitus: Grey matter decrease in auditory and non-auditory brain areas. Neuroimage 46:213–218.
Langguth B, Goodey R, Azevedo A, Bjorne A, Cacace A, Crocetti A, Del Bo L, De Ridder D, Diges I, Elbert T, Flor H, Herraiz C, Ganz Sanchez T, Eichhammer P, Figueiredo R, Hajak G, Kleinjung T, Landgrebe M, Londero A, Lainez MJ, Mazzoli M, Meikle MB, Melcher J, Rauschecker JP, Sand PG, Struve M, Van de Heyning P, Van Dijk P, Vergara R (2007): Consensus for tinnitus patient assessment and treatment outcome measurement: Tinnitus Research Initiative meeting, Regensburg, July 2006. Prog Brain Res 166:525–536.
Leaver AM, Renier L, Chevillet MA, Morgan S, Kim HJ, Rauschecker JP (2011): Dysregulation of limbic and auditory networks in tinnitus. Neuron 69:33–43.
Leaver AM, Seydell-Greenwald A, Turesky TK, Morgan S, Kim HJ, Rauschecker JP (2012): Cortico-limbic morphology separates tinnitus from tinnitus distress. Front Syst Neurosci 6:21.
Leaver AM, Espinoza R, Joshi SH, Vasavada M, Njau S, Woods RPR, Narr KLK (2015a): Desynchronization and plasticity of striato-frontal connectivity in major depressive disorder. Cereb Cortex pii:bhv207.
Leaver AM, Seydell-Greenwald A, Rauschecker JP (2015b): Auditory-limbic interactions in chronic tinnitus: Challenges for neuroimaging research. Hear Res pii:S0378-5955.
Lockwood AH, Salvi RJ, Coad ML, Towsley ML, Wack DS, Murphy BW (1998): The functional neuroanatomy of tinnitus: Evidence for limbic system links and neural plasticity. Neurology 50:114–120.
Maudoux A, Lefebvre P, Cabay J-E, Demertzi A, Vanhaudenhuyse A, Laureys S, Soddu A (2012a): Connectivity graph analysis of the auditory resting state network in tinnitus. Brain Res 1485:10–21.
Maudoux A, Lefebvre P, Cabay J-E, Demertzi A, Vanhaudenhuyse A, Laureys S, Soddu A (2012b): Auditory resting-state network connectivity in tinnitus: A functional MRI study. PLoS One 7:e36222.
McDonald AJ (1987): Organization of amygdaloid projections to the mediodorsal thalamus and prefrontal cortex: A fluorescence retrograde transport study in the rat. J Comp Neurol 262:46–58.
Melcher JR, Sigalovsky IS, Guinan Jr JJ, Levine RA (2000): Lateralized tinnitus studied with functional magnetic resonance imaging: Abnormal inferior colliculus activation. J Neurophysiol 83: 1058–1072.
Melcher JR, Levine RA, Bergevin C, Norris B (2009): The auditory midbrain of people with tinnitus: Abnormal sound-evoked activity revisited. Hear Res 257:63–74.
Melcher JR, Knudson IM, Levine RA (2012): Subcallosal brain structure: Correlation with hearing threshold at supra-

clinical frequencies (>8 kHz), but not with tinnitus. Hear Res 295:1–8.
Mirz F, Gjedde A, Ishizu K, Pedersen CB (2000): Cortical networks subserving the perception of tinnitus–a PET study. Acta Otolaryngol 543:241–243.
Møller AR (2003): Pathophysiology of tinnitus. Otolaryngol Clin North Am 36:249–266.
Mühlau M, Rauschecker JP, Oestreicher E, Gaser C, Röttinger M, Wohlschläger AM, Simon F, Etgen T, Conrad B, Sander D (2006): Structural brain changes in tinnitus. Cereb Cortex 16: 1283–1288.
Newman CW, Jacobson GP, Spitzer JB (1996): Development of the tinnitus handicap inventory. Arch Otolaryngol Head Neck Surg 122:143–148.
Pandya DN, Rosene DL, Doolittle AM (1994): Corticothalamic connections of auditory-related areas of the temporal lobe in the rhesus monkey. J Comp Neurol 345:447–471.
Pawela CP, Biswal BB, Hudetz AG, Li R, Jones SR, Cho YR, Matloub HS, Hyde JS (2010): Interhemispheric neuroplasticity following limb deafferentation detected by resting-state functional connectivity magnetic resonance imaging (fcMRI) and functional magnetic resonance imaging (fMRI). Neuroimage 49:2467–2478.
Perlbarg V, Bellec P, Anton J-L, Pélégrini-Issac M, Doyon J, Benali H (2007): CORSICA: Correction of structured noise in fMRI by automatic identification of ICA components. Magn Reson Imaging 25:35–46.
Plassmann H, O'Doherty JP, Rangel A (2010): Appetitive and aversive goal values are encoded in the medial orbitofrontal cortex at the time of decision making. J Neurosci 30:10799–10808.
Poline JB, Worsley KJ, Evans AC, Friston KJ (1997): Combining spatial extent and peak intensity to test for activations in functional imaging. Neuroimage 5:83–96.
Power JD, Fair DA, Schlaggar BL, Petersen SE (2010): The development of human functional brain networks. Neuron 67:735–748.
Power JD, Barnes KA, Snyder AZ, Schlaggar BL, Petersen SE (2012): Spurious but systematic correlations in functional connectivity MRI networks arise from subject motion. Neuroimage 59:2142–2154.
Raichle ME, MacLeod AM, Snyder AZ, Powers WJ, Gusnard DA, Shulman GL (2001): A default mode of brain function. Proc Natl Acad Sci USA 98:676–682.
Rauschecker JP, Tian B, Hauser M (1995): Processing of complex sounds in the macaque nonprimary auditory cortex. Science 268:111–114.
Rauschecker JP, Leaver AM, Mühlau M (2010): Tuning out the noise: Limbic-auditory interactions in tinnitus. Neuron 66:819–826.
Rauschecker JP, May ES, Maudoux A, Ploner M (2015): Frontostriatal gating of tinnitus and chronic pain. Trends Cogn Sci 19: 567–578.
Ray JP, Price JL (1993): The organization of projections from the mediodorsal nucleus of the thalamus to orbital and medial prefrontal cortex in macaque monkeys. J Comp Neurol 337:1–31.
Roitman MF, Wheeler RA, Carelli RM (2005): Nucleus accumbens neurons are innately tuned for rewarding and aversive taste stimuli, encode their predictors, and are linked to motor output. Neuron 45:587–597.
Romanski LM, Giguere M, Bates JF, Goldman-Rakic PS (1997): Topographic organization of medial pulvinar connections with the prefrontal cortex in the rhesus monkey. J Comp Neurol 379:313–332.
Salimi-Khorshidi G, Douaud G, Beckmann CF, Glasser MF, Griffanti L, Smith SM (2014): Automatic denoising of functional MRI data: Combining independent component analysis and hierarchical fusion of classifiers. Neuroimage 90:449–468.
Satterthwaite TD, Elliott MA, Gerraty RT, Ruparel K, Loughead J, Calkins ME, Eickhoff SB, Hakonarson H, Gur RC, Gur RE, Wolf DH (2013): An improved framework for confound regression and filtering for control of motion artifact in the preprocessing of resting-state functional connectivity data. Neuroimage 64:240–256.
Schlee W, Mueller N, Hartmann T, Keil J, Lorenz I, Weisz N (2009): Mapping cortical hubs in tinnitus. BMC Biol 7:80.
Schmidt SA, Akrofi K, Carpenter-Thompson JR, Husain FT (2013): Default mode, dorsal attention and auditory resting state networks exhibit differential functional connectivity in tinnitus and hearing loss. PLoS One 8:e76488.
Seydell-Greenwald A, Leaver AM, Turesky TK, Morgan S, Kim HJ, Rauschecker JP (2012): Functional MRI evidence for a role of ventral prefrontal cortex in tinnitus. Brain Res 1485:22–39.
Seydell-Greenwald A, Raven EP, Leaver AM, Turesky TK, Rauschecker JP (2014): Diffusion imaging of auditory and auditory-limbic connectivity in tinnitus: Preliminary evidence and methodological challenges. Neural Plast 2014:145943.
Shulman A (1995): A final common pathway for tinnitus - The medial temporal lobe system. Int Tinnitus J 1:115–126.
Shulman A, Goldstein B, Strashun AM (2009): Final common pathway for tinnitus: Theoretical and clinical implications of neuroanatomical substrates. Int Tinnitus J 15:5–50.
Smith SM, Fox PT, Miller KL, Glahn DC, Fox PM, Mackay CE, Filippini N, Watkins KE, Toro R, Laird AR, Beckmann CF (2009): Correspondence of the brain's functional architecture during activation and rest. Proc Natl Acad Sci USA 106:13040–13045.
Talairach TM, Tournoux P (1988): Co-Planar Stereotaxic Atlas of the Human Brain: 3-Dimensional Proportional System: An Approach to Cerebral Imaging. New York: Thieme.
Tanibuchi I, Goldman-Rakic PS (2003): Dissociation of spatial-, object-, and sound-coding neurons in the mediodorsal nucleus of the primate thalamus. J Neurophysiol 89:1067–1077.
Thomas CG, Harshman RA, Menon RS (2002): Noise reduction in bold-based fmri using component analysis. Neuroimage 17: 1521–1537.
Uddin LQ, Kelly AM, Biswal BB, Castellanos FX, Milham MP, Xavier Castellanos F (2009): Functional connectivity of default mode network components: Correlation, anticorrelation, and causality. Hum Brain Mapp 30:625–637.
Van Essen DC, Ugurbil K, Auerbach E, Barch D, Behrens TEJ, Bucholz R, Chang A, Chen L, Corbetta M, Curtiss SW, Della Penna S, Feinberg D, Glasser MF, Harel N, Heath AC, Larson-Prior L, Marcus D, Michalareas G, Moeller S, Oostenveld R, Petersen SE, Prior F, Schlaggar BL, Smith SM, Snyder AZ, Xu J, Yacoub E (2012): The Human Connectome Project: A data acquisition perspective. Neuroimage 62:2222–2231.
Vanneste S, Plazier M, der Loo EV, de Heyning PV, Congedo M, De Ridder D (2010): The neural correlates of tinnitus-related distress. Neuroimage 52:470–480.
Vanneste S, Heyning PVD, Ridder DD (2011a): Contralateral parahippocampal gamma-band activity determines noise-like

tinnitus laterality: A region of interest analysis. Neuroscience 199:481–490.

Vanneste S, van de Heyning P, De Ridder D (2011b): The neural network of phantom sound changes over time: A comparison between recent-onset and chronic tinnitus patients. Eur J Neurosci 34:718–731.

Vanneste S, De Ridder D (2012): The auditory and non-auditory brain areas involved in tinnitus. An emergent property of multiple parallel overlapping subnetworks. Front Syst Neurosci 6:31.

Vanneste S, Congedo M, De Ridder D (2014): Pinpointing a highly specific pathological functional connection that turns phantom sound into distress. Cereb Cortex 24:2268–2282.

Wager TD, Davidson ML, Hughes BL, Lindquist MA, Ochsner KN (2008): Prefrontal-subcortical pathways mediating successful emotion regulation. Neuron 59:1037–1050.

Weiskopf N, Hutton C, Josephs O, Deichmann R (2006): Optimal EPI parameters for reduction of susceptibility-induced BOLD sensitivity losses: A whole-brain analysis at 3 T and 1.5 T. Neuroimage 33:493–504.

Wig GS, Laumann TO, Petersen SE (2014): An approach for parcellating human cortical areas using resting-state correlations. Neuroimage 93:276–291.

Wineland AM, Burton H, Piccirillo J (2012): Functional connectivity networks in nonbothersome tinnitus. Otolaryngol Head Neck Surg 147:900–906.